

## Activation cross section and isomeric cross-section ratio for the $^{46}\text{Ti}(n,p)^{46}\text{Sc}^{m,g}$ process

N. I. Molla\* and S. M. Qaim

*Institut für Chemie I (Nuklearchemie), Forschungszentrum Jülich GmbH, 5170 Jülich, Federal Republic of Germany*

M. Uhl

*Institut für Radiumforschung und Kernphysik, Universität Wien, A-1090 Vienna, Austria*

(Received 9 April 1990)

Excitation functions were measured for the  $^{46}\text{Ti}(n,p)^{46}\text{Sc}^m$  and  $^{46}\text{Ti}(n,p)^{46}\text{Sc}^{m+g}$  reactions over the neutron energy range of 5.4 to 10.5 MeV. Use was made of the activation technique in combination with high-resolution  $\gamma$ -ray spectroscopy. From the available experimental data isomeric cross-section ratios  $[\sigma_m/(\sigma_m + \sigma_g)]$  were determined. Statistical-model calculations taking into account precompound effects were performed for fast neutron-induced reactions on  $^{46}\text{Ti}$ . The calculational results agree well with the experimental data on emitted proton spectra as well as on the excitation functions of various reaction channels. The calculated cross section for the formation of the isomeric state ( $\sigma_m$ ) is strongly dependent on the input level scheme of the product nucleus; the same effect is reflected in the calculation of the isomeric cross-section ratio.

### I. INTRODUCTION

Studies of excitation functions of neutron threshold reactions are of considerable significance for testing nuclear models. Similarly, information on isomeric cross-section ratios, especially as a function of energy, is of great value in studying the effect of nuclear spin. In general, cross sections for the formation of isomeric states are more difficult to predict than those for the total reaction channels. Model calculations on the isomeric states have to account for more details and, furthermore, depend critically on the input level scheme of the residual nucleus (cf. Ref. 1). In this work we chose to investigate the  $^{46}\text{Ti}(n,p)^{46}\text{Sc}^{m,g}$  process. The aim was to test the predictive power of model calculations rather than to attempt reproduction of the experimental data by exploiting the uncertainties of model parameters. It is expected that comprehensive comparisons of experimental and theoretical data would improve the models and their parametrization.

### II. EXPERIMENTAL

Cross sections were measured by the activation technique. Some of the salient features relevant to the present measurements are given below.

#### A. Irradiations and neutron flux monitoring

About 5-g Ti metal powder (>99.9%, Koch-Light, England) was pressed at 10 t/cm<sup>2</sup> and a disc ( $\phi=2$  cm, thickness = 0.5 cm) was obtained. Monitor foils (Al or Fe, each 200  $\mu\text{m}$  thick) were then attached in front and at the back of the sample, and irradiations were done in the 0° direction with quasimonoenergetic neutrons produced via the  $^2\text{H}(d,n)^3\text{He}$  reaction on a D<sub>2</sub> gas target at the Jülich variable energy compact cyclotron CV28. The characteristics of this neutron source have been described earlier (cf. Ref. 2). The average neutron energy effective

at the sample was calculated as described earlier (cf. Refs. 2–4). By varying the primary deuteron energy between 3 and 8 MeV it was possible to vary the neutron energy in the range of 5.4 to 10.5 MeV.

For investigations on the long-lived  $^{46}\text{Sc}^g$  the irradiation time was between 4 and 8 h. The neutron flux density was determined via the monitor reaction  $^{56}\text{Fe}(n,p)^{56}\text{Mn}$  ( $T_{1/2}=2.58$  h,  $E_\gamma=847$  keV,  $I_\gamma=98.87\%$ ) or  $^{27}\text{Al}(n,\alpha)^{24}\text{Na}$  ( $T_{1/2}=15.0$  h,  $E_\gamma=1368$  keV;  $I_\gamma=100\%$ ). The energy region covered by each reaction has been given earlier (cf. Ref. 5). The cross sections of the  $^{56}\text{Fe}(n,p)^{56}\text{Mn}$  reaction were taken from ENDF/B-V (Ref. 6) and those for the  $^{27}\text{Al}(n,\alpha)^{24}\text{Na}$  reaction from Tagesen and Vonach (Ref. 7). The mean neutron flux density was obtained by taking a mean of the flux values from the front and back monitor foils.

In studies on short-lived  $^{46}\text{Sc}^m$  the irradiation time was 2 min. At each neutron energy several successive runs were performed on the same Ti sample but using fresh monitor foils. The neutron flux density was determined via one of the two monitor reactions mentioned above as well as via the  $^{46}\text{Ti}(n,p)^{46}\text{Sc}^g$  reaction whose cross section was determined independently. The two values agreed within 3% and a mean was taken.

#### B. Measurement of radioactivity

The radioactivity of  $^{46}\text{Sc}^g$  ( $T_{1/2}=84.0$  d,  $E_\gamma=889$  and 1121 keV,  $I_\gamma=100\%$  each) was determined via conventional Ge(Li) detector  $\gamma$ -ray spectroscopy several days after the end of irradiation. In the case of  $^{46}\text{Sc}^m$  ( $T_{1/2}=18.7$  s,  $E_\gamma=143$  keV,  $I_\gamma=62.1\%$ ) the sample was quickly transferred from the irradiation position to the detector, and counting was started about 25 s after the end of irradiation. The count rates were corrected for self-absorption, pile-up, and coincidence effects. Due to the low energy of its  $\gamma$ -ray, the self-absorption effect for  $^{46}\text{Sc}^m$  was significant and was determined using an  $^{123}\text{I}$  source ( $E_\gamma=159$  keV). For  $^{46}\text{Sc}^g$ , on the other hand, the

coincidence effect had to be determined carefully. From the count rates, the decay rates were obtained using the  $\gamma$ -ray emission probability (cf. Ref. 8) and the efficiency of the detector which was determined using standard  $\gamma$ -ray sources.

### C. Calculation of cross sections and errors

The decay rates of both  $^{46}\text{Sc}^g$  and  $^{46}\text{Sc}^m$  were corrected for contributions from background neutrons (gas out/gas in results<sup>2</sup> and breakup of deuterons on  $\text{D}_2$  gas<sup>9</sup>). From the corrected decay rates and the mean neutron flux densities the cross sections were calculated using the well-known activation equation. The principal sources of errors and their magnitudes were similar to those in our earlier activation measurements (cf. Refs. 2–4). Combining the individual errors in quadrature, the total error for each cross-section value was obtained.

## III. NUCLEAR MODEL CALCULATIONS

Calculations were performed with the code MAURINA.<sup>10</sup> They considered the statistical (compound-nucleus) model for equilibrium emission, the exciton model for preequilibrium emission and a simple collective model for inelastic scattering.

The statistical model accounted for angular momentum and parity conservation and was supplemented by an appropriate treatment of  $\gamma$ -ray cascades; these features were required for calculation on the isomeric state.

The particle transmission coefficients  $T_{ij}$  were derived from global optical potentials given by Rapaport *et al.*,<sup>11</sup> Mani *et al.*,<sup>12</sup> and McFadden and Satchler<sup>13</sup> for neutrons, protons, and alpha particles, respectively; the neutron potential<sup>11</sup> was modified for lower energies ( $E_n \leq 8$  MeV) in order to improve the reproduction of the total cross sections and the  $s$ - and  $p$ -wave strength functions in this mass region. For the  $\gamma$ -ray transmission coefficients  $T_{XL}$  we used the Brink Axel model<sup>14</sup> in case of  $E1$  radiation and the single particle model<sup>15</sup> for  $T_{M1}, \dots, T_{M3}$  with parameters determined previously for this mass region.<sup>16</sup> It turned out that the results of interest for this paper do not critically depend on these quantities.

The level densities were calculated according to a model proposed by Ignatyuk *et al.*<sup>17</sup> (ISS model). This model accounts for shell effects in terms of the shell correction to the binding energy and considers pairing effects in the frame of a simplified BCS formalism. We did not apply the correction for vibrational enhancement described in Ref. 18 but chose the parameters of the model so as to reproduce available experimental information as far as possible. The asymptotic level density parameter  $a$  was determined by reproducing the experimental average  $s$ -wave resonance spacing  $D_0$  taken from Refs. 19 and 20. For the parameters  $\Delta_0$  (the pairing gap) and  $\gamma$  (determining the energy dependence of the level density parameter) we used the global prescriptions in terms of the mass number  $A$ :  $\Delta_0 = 12/A^{1/2}$  (MeV) and  $\gamma = 0.4/A^{1/3}$  (MeV<sup>-1</sup>). For nuclei with no resonance data we assumed that  $a/A$  is constant in a narrow mass range; an advancement of level density models relying on the shell correc-

tion is the relatively small spread of  $a/A$  (Ref. 19). In the low energy region we supplemented the ISS model by a smoothly joining constant temperature form for the total level density with parameters determined from the number of low-lying levels as prescribed by Gilbert and Cameron.<sup>21</sup> However, we used for all excitation energies the spin cutoff factor  $\sigma$  of the ISS model. This quantity is based on the rigid body moment of inertia; below the critical energy, however,  $\sigma$  is reduced by the pairing correlations. We neglected the parity dependence of the level density. Crude estimates of the impact of this approximation indicated only small effects for the reactions of interest in this paper.

The level schemes of all the relevant nuclei were taken from Nuclear Data Sheets (Refs. 22–24) and Table of Isotopes (Ref. 8). For  $^{46}\text{Sc}$  we explicitly used the first 15 levels of the decay scheme evaluated by Alburger,<sup>24</sup> the continuum starting at 1.14 MeV.

In the exciton model we treated angular momentum conservation in the frame of the mean lifetime ansatz proposed by Shi Xiangjun *et al.*<sup>25</sup> The rates for particle-hole pair creation were calculated according to the method of Oblozinsky *et al.*<sup>26</sup> combined with the expression of Kalbach<sup>27</sup> for the average matrix element of residual interactions with a normalization constant  $K' = 130$  MeV<sup>3</sup>. The nucleon emission rates were calculated according to Gadioli *et al.*<sup>28</sup> while for alpha particles we used the model of preformed alpha clusters proposed by Milazzo-Colli and Braga-Marcazzan<sup>29</sup> with a preformation factor  $\phi = 0.3$ .

For the state densities with fixed number of excited particles and holes we used the expression given by Williams<sup>30</sup> supplemented by a conventional pairing shift of the size  $\Delta = 12/A^{1/2}$  (MeV). The single particle state density was calculated as  $g = A/13.16$  (MeV<sup>-1</sup>) and the exciton number ( $n$ ) dependent spin cutoff factor as  $\sigma(n)^2 = 0.160nA^{2/3}$  (Ref. 31).

The exciton model parametrized in this way was applied in previous work (mostly in an angular momentum independent formulation) to reproduce a variety of cross sections in this mass region (cf., e.g., Refs. 32–34). The target  $^{46}\text{Ti}$  has a low neutron excess and hence proton emission is favored by the  $Q$  value. Therefore, and also due to the relatively small incident energies, the  $^{46}\text{Ti}(n,px)$  cross sections do not depend very critically on the assumptions regarding preequilibrium decay.

For the treatment of direct inelastic scattering we employed macroscopic collective form factors. We applied the distorted-wave Born approximation and used deformation parameters compiled by Alburger.<sup>24</sup> In our simple model the only effect of direct inelastic scattering on the considered  $(n,p)$  and analogous cross sections is to reduce them by a few percent (e.g., 7% at  $E_n = 15$  MeV) because of flux conservation.

## IV. RESULTS AND DISCUSSION

Measurements were done at seven neutron energies between 5.4 and 10.5 MeV and the cross-section data are presented in Table I. In the case of  $^{46}\text{Ti}(n,p)^{46}\text{Sc}^m$  reaction the total error amounts to between 14% and 19%;

TABLE I. Fast neutron-induced activation cross sections.

Mean neutron energy effective at Ti sample <sup>a</sup> (MeV)	Reaction cross section (mb)	
	$^{46}\text{Ti}(n,p)^{46}\text{Sc}^m$	$^{46}\text{Ti}(n,p)^{46}\text{Sc}^{m+g}$
5.37±0.24	46.0±8.6	87.0±8.9
6.48±0.27	71.5±9.8	157.6±17.1
7.52±0.31	86.2±11.9	197.6±18.6
8.53±0.31	97.9±14.7	255.9±26.1
9.49±0.39	108.2±16.6	260.6±33.3
9.98±0.40	104.4±15.4	287.5±33.6
10.47±0.39	118.0±19.6	315.0±37.5

<sup>a</sup>The deviations do not give errors; they show energy spreads due to angle of emission.

19%; for  $^{46}\text{Ti}(n,p)^{46}\text{Sc}^{m+g}$  it is between 9 and 13%. Over the reported energy range the cross sections for the  $^{46}\text{Ti}(n,p)^{46}\text{Sc}^m$  reaction have been measured for the first time.

As a check on the model calculations, we first discuss the results on the proton and alpha particle emission spectra. The experimental proton emission spectrum reported by Grimes *et al.*<sup>35</sup> for 15-MeV neutrons incident on  $^{46}\text{Ti}$  is given in Fig. 1 together with our calculational results. The good agreement at the high energy end of the proton spectrum confirms the proper choice of the exciton model parameters, and the good description of the bump at low emission energies indicates that the  $(n,np)$  reaction is also reproduced. The alpha particle emission, however, was not described very well, our

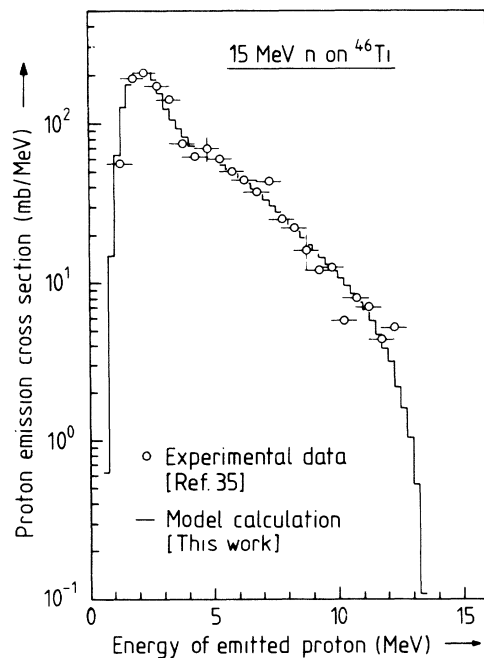


FIG. 1. Experimentally determined angle-integrated cross sections for proton emission in the interactions of 15-MeV neutrons with  $^{46}\text{Ti}$  (Ref. 35), and comparison with the results of statistical-model calculation (this work).

theoretical values being about 30% smaller than the experimental data.<sup>35</sup> These deviations are larger than those found in previous work on  $(n,\alpha)$  reactions on target nuclei  $^{55}\text{Mn}$ ,  $^{56}\text{Fe}$ ,  $^{59}\text{Co}$ , and  $^{58,60}\text{Ni}$  (cf. Refs. 32, 36, and 37). This may be due to several reasons: for example, failure of the simple model of preformed alpha clusters (Ref. 29) for smaller mass numbers. However, since alpha emission represents only a small fraction of the absorption cross section, deficiencies in the treatment of the alpha channel hardly affect the  $(n,px)$  and  $(n,nx)$  cross sections.

As a next step, a comparison of experimental and calculated excitation functions was undertaken. Our calculations reproduced the experimental  $^{46}\text{Ti}(n,2n)^{45}\text{Ti}$  excitation function very well. The results for the  $^{46}\text{Ti}(n,p)^{46}\text{Sc}^{m+g}$  process are given in Fig. 2. Several experimental reports existed on this reaction (cf. Refs. 38–44). Our experimental data agree with the literature values and slightly extend the energy scale of measurements with *dd* neutrons. Beyond 15 MeV the data base is weak, the only real  $(n,p)$  values being those of Pai.<sup>40</sup> Other experimental values (cf. Ref. 38) consist of summed  $(n,p)$  and  $(n,n'p)$  contributions. The evaluated curve (ENDF/B-V) used for dosimetry purposes is also given. Our calculated results show satisfactory agreement with the experimental data, especially in view of the fact that no adjustment of the level-density parameters was done (those for  $^{46}\text{Ti}$  and  $^{45}\text{Ti}$  rely on systematics of  $\bar{a}$ ).

The cross-section data for the  $^{46}\text{Ti}(n,p)^{46}\text{Sc}^m$  reaction are given in Fig. 3. For this reaction a few experimental cross-section values were available in the 14 to 15 MeV region (cf. Refs. 44–46) but near the threshold no data existed. The reasonable reproduction of the data by the calculation employing the ISS model for the level density (full curve) is mainly due to the reduction of the spin cutoff factor below the critical energy by pairing. In order to achieve a comparable fit with the back-shifted

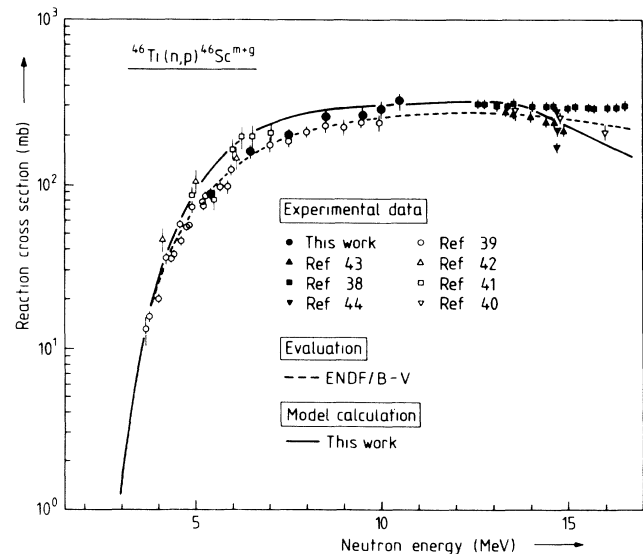


FIG. 2. Excitation function of the  $^{46}\text{Ti}(n,p)^{46}\text{Sc}^{m+g}$  process. The solid curve gives the results of model calculation.

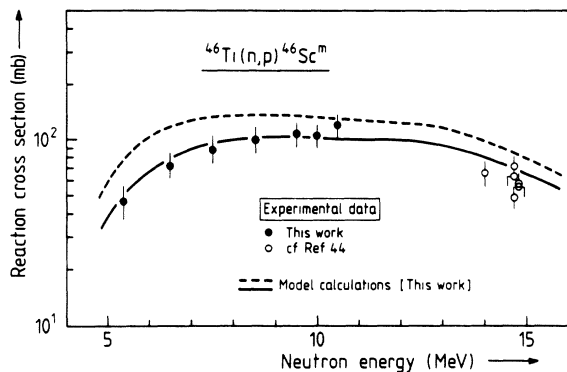


FIG. 3. Excitation function of the  $^{46}\text{Ti}(n,p)^{46}\text{Sc}^m$  reaction. The solid curve gives the results of model calculation taking into account 15 discrete levels of the product nucleus  $^{46}\text{Sc}$ ; the dashed curve describes calculational results considering only the first 8 levels.

Fermi-gas model<sup>47</sup> one has to assume a moment of inertia that is reduced (for all excitation energies) by a factor of more than 2 compared to the rigid body value. Of course, before claiming a definite advantage of the ISS model, more cases should be studied. In particular, since the ISS model uses a very simple prescription to treat pairing in odd  $A$  and in odd-odd nuclei, such studies should involve isomers in nuclei of different types. Finally we would like to emphasize that conclusions on the level density model are complicated by the critical dependence of isomeric state population cross section ( $\sigma_m$ ) on uncertainties in the level scheme of the product nucleus. As a simple illustration we show in Fig. 3 (as a dashed curve) the results obtained if explicitly only the first 8 levels are taken into account instead of the first 15 levels considered for the solid curve.

The isomeric cross-section ratios  $[\sigma_m / (\sigma_m + \sigma_g)]$  deduced from the experimental cross-section data as well as from the model calculations are shown in Fig. 4. The ratio is somewhat high at low incident neutron energies, but decreases with increasing energy, reaching a value of

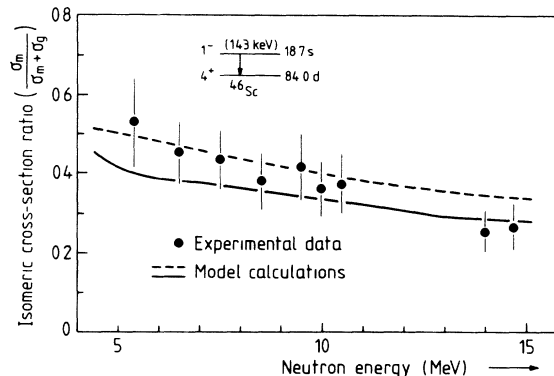


FIG. 4. Isomeric cross-section ratio for the isomeric pair  $^{46}\text{Sc}^{m,8}$  [formed via  $(n,p)$  reaction on  $^{46}\text{Ti}$ ] plotted as a function of incident neutron energy. The solid and dashed curves give results of model calculations, taking into account 15 or 8 discrete levels of the product nucleus  $^{46}\text{Sc}$ , respectively.

about 0.27 at 14.5 MeV. This behavior may be understood in terms of the spins of the two states concerned. The results of model calculations done for two cases, viz., input of only 8 or 15 levels of the product nucleus, agree with the experimental isomeric cross-section ratios in general within the limits of experimental errors. The deviations between the two theoretical curves, however, should emphasize the importance of input level scheme of the product nucleus on the isomeric cross-section ratio.

#### ACKNOWLEDGMENTS

The Jülich authors thank Professor G. Stöcklin for his active support of the experimental work. N. I. Molla thanks the Commission of the European Communities for a fellowship. All the calculations were performed on an IBM 3090-400E VF computer installed at the University of Vienna in the frame of the European Academic Supercomputing Initiative (EASI) of IBM Corporation. The help given by the staff of the Vienna University Computer Centre is acknowledged.

\*Present address: Institute of Nuclear Science and Technology, Atomic Energy Research Establishment, Dhaka, Bangladesh.

<sup>1</sup>S. M. Qaim, A. Mushtaq, and M. Uhl, *Phys. Rev. C* **38**, 645 (1988).

<sup>2</sup>S. M. Qaim, R. Wölffe, M. M. Rahman, and H. Ollig, *Nucl. Sci. Eng.* **88**, 143 (1984).

<sup>3</sup>A. Suhaimi, R. Wölffe, S. M. Qaim, and G. Stöcklin, *Radiochimica Acta* **40**, 113 (1986).

<sup>4</sup>S. M. Qaim and R. Wölffe, *Nucl. Sci. Eng.* **96**, 52 (1987).

<sup>5</sup>M. Ibn Majah and S. M. Qaim, *Nucl. Sci. Eng.* **104**, 271 (1990).

<sup>6</sup>Evaluated Nuclear Data File (ENDF)/B-V, Dosimetry File (1979), issued by National Nuclear Data Center, Brookhaven National Laboratory, received as computer listing in Nuclear Energy Agency Data Bank, Saclay, France.

<sup>7</sup>S. Tagesen and H. Vonach, *Physics Data 13-3* (Fachinformationszentrum, Karlsruhe, 1981); see also H. Vonach, International Atomic Energy Agency, Technical Report Series No. 227 (IAEA Vienna, 1983), p. 59.

<sup>8</sup>*Table of Isotopes*, 7th ed., edited by C. M. Lederer and V. S. Shirley (Wiley, New York, 1978).

<sup>9</sup>J. W. Meadows and D. L. Smith, "Neutron source investigations in support of the cross section program at the Argonne fast neutron generator," ANL Report ANL/NDM-53 (1980).

<sup>10</sup>M. Uhl, Institut für Radiumforschung und Kernphysik, University of Vienna (unpublished).

<sup>11</sup>J. Rapaport, V. Kulkarni, and R. W. Finlay, *Nucl. Phys.* **A330**, 15 (1979).

<sup>12</sup>G. S. Mani, M. A. Melkanoff, and I. Iori, CEA Report CEA-

- 2379, 1963 (unpublished).
- <sup>13</sup>L. McFadden and G. R. Satchler, *Nucl. Phys.* **84**, 177 (1966).
- <sup>14</sup>D. M. Brink, Ph.D. thesis, Oxford University, 1955; P. Axel, *Phys. Rev.* **126**, 671 (1962).
- <sup>15</sup>J. M. Blatt and V. F. Weisskopf, *Theoretical Nuclear Physics* (Wiley, New York, 1952).
- <sup>16</sup>B. Strohmaier and M. Uhl, *Proceedings of the International Conference on Nuclear Data for Science and Technology*, Antwerp, 1982, edited by K.-H. Böckhoff (Reidel Publishing Company, Dordrecht, 1983), p. 552.
- <sup>17</sup>A. V. Ignatyuk, K. K. Istekov, and G. N. Smirenkin, *Yad. Fiz.* **29**, 875 (1979) [*Sov. J. Nucl. Phys.* **29**, 450 (1979)].
- <sup>18</sup>O. T. Grudzevich, A. V. Ignatyuk, V. I. Plyaskin, and A. V. Zelenetsky, *Proceedings of the International Conference on Nuclear Data for Science and Technology*, Mito, Japan, 1988, edited by S. Igavasi (Saikon, Tokyo, 1988), p. 767.
- <sup>19</sup>H. Vonach, M. Uhl, B. Strohmaier, B. W. Smith, E. G. Bilpuch and G. E. Mitchell, *Phys. Rev.* **C38**, 2451 (1988).
- <sup>20</sup>S. F. Mughabgab, M. Divadeenam, and N. E. Holden, *Neutron Cross Sections* (Academic, New York, 1981), Vol. 1, Part A.
- <sup>21</sup>A. Gilbert and A. G. W. Cameron, *Can. J. Phys.* **43**, 1446 (1965).
- <sup>22</sup>T. W. Burrows, *Nucl. Data Sheets* **40**, 149 (1983).
- <sup>23</sup>T. W. Burrows, *Nucl. Data Sheets* **48**, 1 (1986).
- <sup>24</sup>D. E. Alburger, *Nucl. Data Sheets* **49**, 237 (1986).
- <sup>25</sup>Shi Xiangjun, H. Gruppelaar, and J. M. Akkermans, *Nucl. Phys.* **A466**, 333 (1987).
- <sup>26</sup>P. Oblozinsky, I. Ribansky, and E. Betak, *Nucl. Phys.* **A226**, 347 (1974).
- <sup>27</sup>C. Kalbach, *Z. Phys. A* **287**, 319 (1978).
- <sup>28</sup>E. Gadioli, E. Erba-Gadioli, and P. G. Sona, *Nucl. Phys.* **A217**, 589 (1973).
- <sup>29</sup>L. Milazzo-Colli and G. Braga-Marcuzzan, *Nucl. Phys.* **A210**, 297 (1973).
- <sup>30</sup>F. C. Williams Jr., *Nucl. Phys.* **A166**, 231 (1971).
- <sup>31</sup>H. Feshbach, A. K. Kerman, and S. Koonin, *Ann. Phys.* (N.Y.) **125**, 429 (1980).
- <sup>32</sup>A. Pavlik, G. Winkler, M. Uhl, A. Paulsen, and H. Liskien, *Nucl. Sci. Eng.* **90**, 186 (1985).
- <sup>33</sup>S. J. Hasan, A. Pavlik, G. Winkler, M. Uhl, and G. Kaba, *J. Phys. G* **12**, 397 (1986).
- <sup>34</sup>H. Liskien, M. Uhl, M. Wagner, and G. Winkler, *Ann. Nucl. Energy* (in press).
- <sup>35</sup>S. M. Grimes, R. C. Haight, and J. D. Anderson, *Nucl. Sci. Eng.* **62**, 187 (1977).
- <sup>36</sup>R. Fischer, G. Traxler, M. Uhl, and H. Vonach, *Phys. Rev.* **C30**, 72 (1984).
- <sup>37</sup>R. Fischer, G. Traxler, M. Uhl, H. Vonach, and P. Maier-Komor, *Phys. Rev.* **C34**, 460 (1986).
- <sup>38</sup>H. Liskien and A. Paulsen, *Nucl. Phys.* **63**, 393 (1965).
- <sup>39</sup>D. L. Smith and J. W. Meadows, *Nucl. Sci. Eng.* **58**, 314 (1975).
- <sup>40</sup>H. H. Pai, *Can. J. Phys.* **44**, 2337 (1966).
- <sup>41</sup>Y. Lukic, *Nucl. Sci. Eng.* **43**, 233 (1971).
- <sup>42</sup>S. K. Ghorai, J. R. Cooper, J. D. Moore, and W. L. Alford, *J. Nucl. Energy* **25**, 319 (1971).
- <sup>43</sup>Y. Ikeda, C. Konno, K. Oishi, T. Nakamura, H. Miyade, K. Kawade, H. Yamamoto, and T. Katoh, *Japan Atomic Energy Research Institute Report JAERI-1312* (1988).
- <sup>44</sup>V. McLane, C. L. Dunford, and P. F. Rose, *Neutron Cross Sections* (Academic, New York, 1988), Vol. 2.
- <sup>45</sup>N. I. Molla and S. M. Qaim, *Nucl. Phys.* **A283**, 269 (1977).
- <sup>46</sup>I. Ribansky and S. Gmuca, *J. Phys. G* **9**, 1537 (1983).
- <sup>47</sup>W. Dilg, W. Schantl, H. Vonach, and M. Uhl, *Nucl. Phys.* **A217**, 269 (1973).